Biochimica et Biophysica Acta 1850 (2015) 435–446

Contents lists available at ScienceDirect

Biochimica et Biophysica Acta

journal homepage: www.elsevier.com/locate/bbagen

Triamcinolone regulated apopto-phagocytic gene expression patterns in the clearance of dying retinal pigment epithelial cells. A key role of Mertk in the enhanced phagocytosis

Réka Albert [a,b,1], Endre Kristóf [b,1], Gábor Zahuczky [c], Mária Szatmári-Tóth [b], Zoltán Veréb [a,b], Brigitta Oláh [a,b], Morten C. Moe [d], Andrea Facskó [a], László Fésüs [b], Goran Petrovski [a,b,*]

[a] Department of Ophthalmology, Faculty of Medicine, University of Szeged, Szeged, Hungary
[b] Stem Cells and Eye Research Laboratory, Department of Biochemistry and Molecular Biology, and MTA-DE Stem cell, Apoptosis and Genomics Research Group, University of Debrecen, Debrecen, Hungary
[c] UD Genomed Ltd., Debrecen, Hungary
[d] Centre of Eye Research, Department of Ophthalmology, Oslo University Hospital, University of Oslo, Oslo, Norway

ARTICLE INFO

Article history:
Received 23 June 2014
Received in revised form 3 October 2014
Accepted 22 October 2014
Available online 27 October 2014

Keywords:
AMD
Anoikis
Phagocytosis
Triamcinolone
MERTK
Gas6

ABSTRACT

Background: The apopto-phagocytic gene expression patterns during clearance of dying cells in the retina and the effect of triamcinolone (TC) upon these processes have relevance to development of age-related macular degeneration (AMD).
Methods: ARPE-19 cells and primary human retinal pigment epithelium (hRPE) were induced to undergo cell death by anoikis and the clearance of these cells by living hRPE/ARPE-19 or human monocyte-derived macrophages (HMDMs) in the presence or absence of TC was quantified by flow cytometry. TaqMan low-density gene expression array determining known markers of phagocytosis and loss-of-function studies on selected apopto-phagocytic genes was carried out in HMDM engulfing anoikic cells.
Results: The glucocorticoid TC had a profound phagocytosis-enhancing effect on HMDM engulfing anoikic ARPE-19 or hRPE cells, causing a selective upregulation of the Mer tyrosine kinase (MERTK) receptor, while decreasing the expression of the AXL receptor tyrosine kinase and thrombospondin-1 (THSB-1). The key role of the MERTK could be demonstrated in HMDM engulfing dying cells using gene silencing as well as blocking antibodies. Similar pathways were found upregulated in living ARPE-19 engulfing anoikic ARPE-19 cells. Gas6 treatment enhanced phagocytosis in TC-treated HMDMs.
Conclusions: Specific agonists of the Mertk receptor may have a potential role as phagocytosis enhancers in the retina and serve as future targets for AMD therapy.
General significance: The use of Gas6 as enhancer of retinal phagocytosis via the MerTK receptor, alone or in combination with other specific ligands of the tyrosine kinase receptors' family may have a potential role in AMD therapy.

1. Introduction

The elimination of dying cells in the retina is performed mainly by the viable retinal pigment epithelial (RPE) cells under intact barrier conditions [1]. Failure of dead cells' clearance may result in drusen accumulation between the RPE and basement (Bruch's) membrane of the retina, which together with the aggregate formation within the RPE are hallmarks of the dry type of age-related macular degeneration (AMD) [2]. Presence of subretinal neovascularization (NV) found in the wet type of AMD involves the mononuclear phagocyte system in the clearance of dying cells [2,3].

The process of apoptotic cell corpse removal by both professional and non-professional phagocytes (macrophages and RPE cells, respectively) is remarkably complex and only partly defined [4,5]. It consists of tethering and tickling steps, which ultimately lead to recognition and engulfment of the apoptotic cells [6]. The so called “third synapse” between the dying cells and the phagocyte involves appearance of ligands or “eat-me” signals on the apoptotic cells as well as bridging molecules and receptors on the phagocytes [7,8]. While many redundant elements of the recognition and receptor elements of the apopto-phagocytic machinery have been described in different organ systems [9], most of them seem to converge onto the rac-1 dependent cytoskeletal pathway [7].

* Corresponding author at: Department of Ophthalmology, University of Szeged, Korányi fasor 10-11, 6720 Szeged, Hungary. Tel.: +36 62 544 573; fax: +36 62 545 487.
E-mail address: petrovski.goran@med.u-szeged.hu (G. Petrovski).
[1] These authors contributed equally in this work.

http://dx.doi.org/10.1016/j.bbagen.2014.10.026
0304-4165/

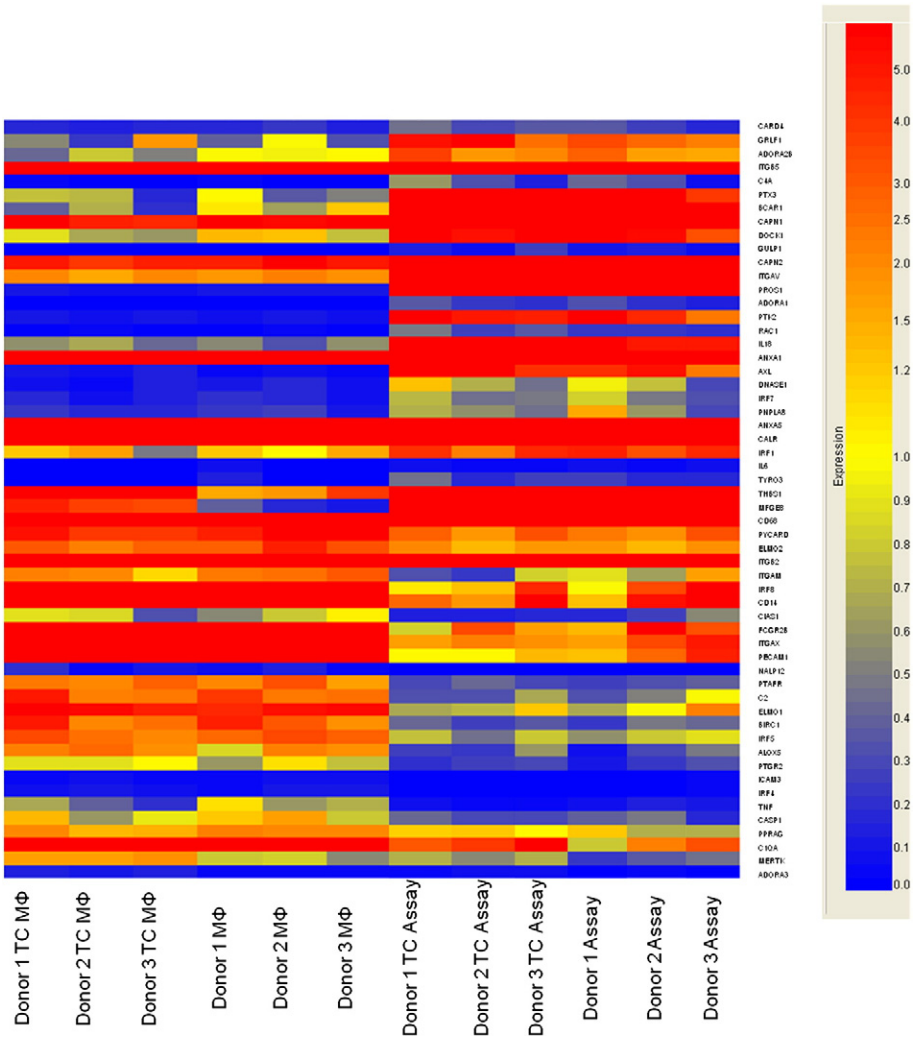

Fig. 1. Heatmap of the 56 genes with significant interdonor changes determined by multiple comparison of the four different groups (Control MΦ, Control Assay vs. TC MΦ, TC Assay).

Corticosteroids (CSs) have been extensively used in different systems for their rapid and delayed effects on physiological and pathological functions. In the eye, the CS triamcinolone (TC)[2] is applied intravitreally for its basic anti-inflammatory, anti-permeability and anti-fibrotic properties [10–12] for treating conditions like diabetic macular edema [13,14]. All CSs exert their action via cytosolic CS receptors which move into the nucleus to regulate gene expression or upon ligand binding to membrane-bound CS receptors [15,16]. The potentiating effect of CS on the phagocytosis of apoptotic neutrophils has been described previously [17–19], and only recently, we have shown the same enhancing effect of TC on the phagocytosis of dying RPE by macrophages. In the first case, the enhanced phagocytic uptake of apoptotic neutrophils has been attributed to the increased engulfment oriented reorganization of cytoskeletal elements, loss of phosphorylation of adhesion mediators (paxillin and pyk2) and increased amount of Rac GTPase [20,21]. Microarray analysis of the expression patterns of CS-induced human monocytes has identified specific gene-clusters as possible functional markers of the anti-inflammatory response: upregulated antioxidative, migration/chemotaxis, phagocytosis, anti-inflammatory genes and down-regulated T-cell chemotaxis, adhesion, apoptosis, oxidative functions and interferon gamma (IFNã) regulated genes [22]. The importance of the tyrosine kinase (Tyro3/Axl/Mer) family of receptors in the phagocytosis of apoptotic cells has been clearly demonstrated in dexamethasone-treated human monocyte derived macrophages (HMDMs) which exhibit augmented capacity of phagocytosis in the presence of protein S, a ligand for Mer tyrosine kinase (MerTk) [23,24].

To the best our knowledge, neither a microarray analysis nor tyrosine kinase receptor involvement studies have been made so far characterizing the phagocytosis enhancing effect of TC in the retina. We therefore investigated the effects of TC on the gene expression pattern of RPE and differentiated HMDMs using a custom designed apoptophagocytic panel [17].

2. Materials and methods

2.1. Cell preparation and culturing, ethics statement

Adult retinal pigment epithelium-19 (ARPE-19) cells were kindly provided by Prof. Stephen Moss, (UCL, London, UK) and cultured in Dulbecco's modified Eagle's medium (DMEM) (Sigma-Aldrich, St. Louis, MO, USA) supplemented with 10% Fetal bovine serum (FBS) (Sigma-Aldrich), 200 mM/mL L-glutamine (Sigma-Aldrich) and 1% Antibiotic/antimycotic solution (PAA, Pasching, Austria).

Human primary RPE (hRPE) cells were isolated from cadavers as described previously [25] and cultured in DMEM Nutrient mixture F12 HAM medium supplemented with 10% FBS (Sigma-Aldrich), 200 mM/mL L-glutamine (Sigma-Aldrich) and 1% Antibiotic/antimycotic solution (PAA, Pasching, Austria).

Table 1
List of genes with significant interdonor changes determined by multiple comparisons of the 4 different groups (Control MΦ, Control Assay vs. TC MΦ, TC Assay).

Gene symbol	Gene description	p-Value
CARD4	Nucleotide-binding oligomerization domain containing 1	0.04890
ADORA2B	Adenosine A2b receptor	0.04500
CD68	CD68 molecule	0.04490
PYCARD	PYD and CARD domain containing	0.04050
ANXA5	Annexin A5	0.03750
GRLF1	Glucocorticoid receptor DNA binding factor 1	0.03610
ITGB2	Integrin, beta 2 (complement component 3 receptor 3 and 4 subunit)	0.03520
FCGR2B	Fc receptor, IgG, low affinity IIb	0.03420
ELMO2	Engulfment and cell motility 2	0.03370
ITGAM	Integrin, alpha M (complement component 3 receptor 3 subunit)	0.03250
ITGB5	Integrin, beta 5	0.03020
IRF8	Interferon regulatory factor 8	0.02950
CALR	Calreticulin	0.02590
THBS1	Thrombospondin 1	0.02540
CD14	CD14 molecule	0.02450
CASP1	Caspase 1	0.02330
DNASE1	Deoxyribonuclease I	0.02250
IRF7	Interferon regulatory factor 7	0.01900
ALOX5	Arachidonate 5-lipoxygenase	0.01900
C4A	Complement component 4A (Rodgers blood group)	0.01650
NALP12	NLR family, pyrin domain containing 12	0.01560
PNPLA8	Patatin-like phospholipase domain containing 8	0.01450
IRF1	Interferon regulatory factor 1	0.01090
C2	Complement component 2	0.00865
C1QA	Complement component 1, q subcomponent, A chain	0.00850
ICAM3	Intercellular adhesion molecule 3	0.00843
CIAS1	NLR family, pyrin domain containing 3	0.00815
PTX3	Pentraxin 3, long	0.00712
CAPN1	Calpain 1, (mu/I) large subunit	0.00706
PPARG	Peroxisome proliferator-activated receptor gamma	0.00455
MFGE8	Milk fat globule-EGF factor 8 protein	0.00453
BIRC1	NLR family, apoptosis inhibitory protein	0.00448
PTGER2	Prostaglandin E receptor 2 (subtype EP2), 53 kDa	0.00409
ELMO1	Engulfment and cell motility 1	0.00365
IRF4	Interferon regulatory factor 4	0.00365
TNF	Tumor necrosis factor	0.00325
IRF5	Interferon regulatory factor 5	0.00239
DOCK1	Dedicator of cytokinesis 1	0.00222
GULP1	GULP, engulfment adaptor PTB domain containing 1	0.00189
MERTK	c-Mer proto-oncogene tyrosine kinase	0.00174
ADORA3	Adenosine A3 receptor	0.00165
BCAR1	Breast cancer anti-estrogen resistance 1	0.00155
IL6	Interleukin 6 (interferon, beta 2)	0.00145
ITGAX	Integrin, alpha X (complement component 3 receptor 4 subunit)	0.00129
PECAM1	Platelet/endothelial cell adhesion molecule 1	0.00124
CAPN2	Calpain 2, (m/II) large subunit	0.00119
TYRO3	TYRO3 protein tyrosine kinase 3	0.00078
PTAFR	Platelet-activating factor receptor	0.00039
ANXA1	Annexin A1	0.00038
ITGAV	Integrin, alpha V	0.00038
AXL	AXL receptor tyrosine kinase	0.00035
IL18	Interleukin 18 (interferon-gamma-inducing factor)	0.00030
ADORA1	Adenosine A1 receptor	0.00027
RAC1	Ras-related C3 botulinum toxin substrate 1 (rho family, small GTP binding protein Rac1)	0.00024
PTK2	PTK2 protein tyrosine kinase 2	0.00013
PROS1	Protein S (alpha)	0.00006

Human monocytes were isolated from 'buffy coats' of healthy blood donors by Ficoll-Paque Plus (Amersham Biosciences, Uppsala, Sweden) gradient and magnetic separation using CD14 human microbeads (Miltenyi Biotec, Auburn, CA, USA). Human macrophages were obtained through a 5-day differentiation using 5 ng/mL macrophage colony-stimulating factor (M-CSF) (Peprotech EC, London, UK) at 37 °C and at a cell density of 1×10^6 cells/mL in Iscove's Modified Dulbecco's Medium (IMDM) (Gibco) containing 10% human AB serum (Sigma-Aldrich) and 10,000 U/mL penicillin–10 mg/mL streptomycin (Sigma-Aldrich).

Buffy coats were provided anonymously by the Hungarian National Blood Service where blood was taken from healthy volunteers and written informed consent from all participants was obtained. For these studies approval was obtained from the ethics committee of the Medical and Health Science Center, University of Debrecen (DEOEC RKEB/IKEB Prot. No. 2745–2008 and 3093–2010). The ethics committee approved this consent procedure.

2.2. Cell treatments, apoptosis and phagocytosis quantification assays

Pre-treatment of macrophages and living ARPE-19 cells with 1 μM TC (Sigma-Aldrich) was performed 48 h prior to the assay. Dying ARPE-19 or hRPE cells were fed to engulfing cells 24 h after the induction of cell death by detachment from the extracellular matrix (anoikis) using poly-2-hydroxyethylmethacrylate (polyHEMA)-coated culture plates. Cell death was assessed by the Annexin-V-fluorescein isothiocyanate Apoptosis Detection Kit (MBL, Woburn, MA, USA) according to manufacturer's recommendations; the proportion of stained Annexin-V^+ and Annexin-V^+/propidium iodide + (PI^+) cells was determined by fluorescence activated cell sorter (FACS) analysis on BD Bioscience flow cytometer. The phagocytes were stained with 7.5 mM 5-(and-6)-(((4-chloromethyl)benzoyl)amino)tetramethylrhodamine (CMTMR) for 16 h and washed twice in phosphate-buffered saline (PBS) before starting the assay. Accordingly, the cells to be engulfed were stained with 12.5 mM of 5-carboxyfluorescein diacetate (CFDA) for 16 h before the phagocytosis and washed twice in PBS before being added to the phagocytes. The ratio of phagocytes and cells to be engulfed was set at 1:2 for the dying hRPE cells and 1:5 for the dying ARPE-19 cells. The phagocytosis assay started when the cells to be engulfed were added to the appropriate phagocytes and kept together for 4 h as determined previously [26]. Where noted, macrophages were pre-incubated with anti-MerTk blocking antibody (R&D systems, Minneapolis, USA) for 10 min at a concentration of 10 μg/mL or with Gas6 (R&D systems) for 24 h at 200 ng/mL concentration before adding the dying cells. The assay was ended by trypsinizing the phagocytic cell mixture to remove bound but not engulfed dying cells, centrifuging, washing twice in PBS and fixing in 1% PBS-buffered paraformaldehyde (pH 7.4). The phagocytosis rate was determined by FACS analysis (BD Bioscience) as percent phagocytic cells ($CMTMR^+$) that have engulfed dying cells ($CMTMR^+CFDA^+$) [26].

2.3. RNA preparation and TaqMan real-time RT-PCR

Total cellular RNA was isolated from untreated and TC-treated HMDMs using TRIzol Reagent (Invitrogen Life Technologies). Total RNA concentrations were quantified by spectrometry after DNase treatment (Sigma-Aldrich). TaqMan reverse transcription reagent kit (Applied Biosystems) was used for generating cDNA according to manufacturer's instructions. Predesigned, factory-loaded 384-well TaqMan low-density array (Applied Biosystems, Foster City, CA, USA) was used to determine the level of expression of genes listed previously [17]. Measurements were carried out using two technical replicates. Expression levels of target genes were normalized to human cyclophyllin as endogenous control.

Table 2
List of genes with significant expression changes in HMDMs during TC treatment (TC MΦ vs Cont MΦ)(FC > 2, $p < 0.05$).

Upregulated genes	FC	p-Value
MFGE8	22.69	0.0129
THBS1	6.31	0.0137
ADORA3	3.95	0.0042
MERTK	2.42	0.0127

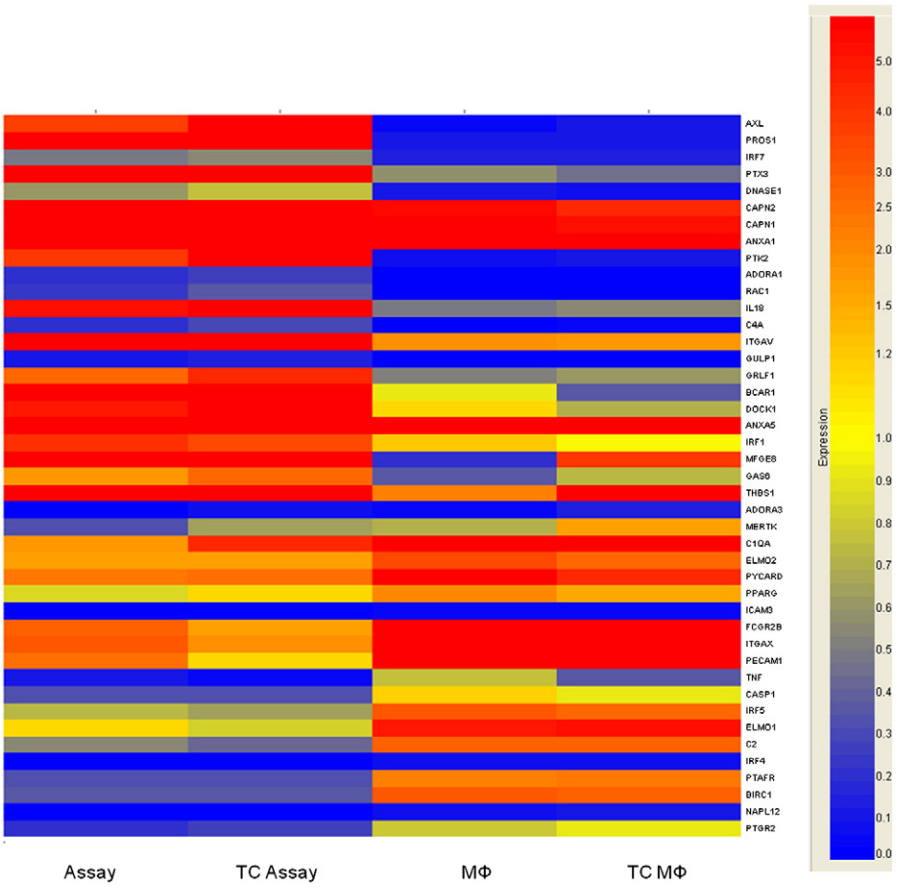

Fig. 2. Heatmap of the 43 out of the 95 genes investigated with significant changes during the assay conditions.

An ABI Prism 7700 sequence detection system (Applied Biosystems) was used to determine relative gene expression analyzing knock-down effect in HMDMs. Gene primers and probes were designed and supplied by Applied Biosystems. Human cyclophyllin was used as endogenous control. All samples were run in triplicates. Gene expression values were calculated based on the ΔΔCt method, where one sample was designated as calibrator, through which all other samples were analyzed. ΔCt represents the threshold cycle (Ct) of the target minus that of hCYC and ΔΔCt represents the ΔCt of each target minus that of the calibrator. Relative quantities (or fold changes) were determined using the equation where relative quantity equals 2 − ΔΔCt.

2.4. siRNAs and electroporation of HMDMs

In order to knock-down each investigated gene, small interfering ribonucleic acid (siRNA) constructs were obtained from Ambion (Life Technologies), targeting adenosine A3 receptor (ADORA3) [3′-CGUCUAUGCCUAUAAAAUAtt (sense) and 5′-UAUUUUAUAGGCAUAGACGtt (antisense)], AXL receptor tyrosine kinase [3′-GGAACUGCAUGCUGAAUGAtt (sense) and 5′-UCAUUCAGCAUGCAGUUCCtg (antisense)], c-mer proto-oncogene tyrosine kinase (MERTK) [3′-GAACUUACCUUACAUAGCUtt (sense) and 5′-AGCUAUGUAAGGUAAGUUCaa (antisense)] and thrombospondin-1 (THBS1) [3′-GGACUGCGUUGGUGAUGUAtt (sense) and 5′- UACAUCACCAACGCAGUCCtt (antisense)]. Non-targeting siRNA negative control (scrambled) was obtained from Sigma-Genosys (3781976-F/112). Three days after isolation, HMDMs and living ARPE-19 cells were harvested from the 24 well plates and washed once with IMDM or DMEM accordingly and once with PBS (all at room temperature). The cells were resuspended in OptiMEM without phenol red (Invitrogen Life Technologies) at a concentration of 4 × 107/mL. siRNA was transferred to a 4-mm cuvette (3 μM final concentration or as indicated). A volume of 100 μL of cell suspension was added and incubated for 3 min before being pulsed in a Genepulser Xcell (Bio-Rad). Pulse conditions were square-wave pulse, 500 V, 0.5 ms for HMDMs [17] and 250 V, 10 ms for non-dying ARPE-19 cells [27]. Immediately after electroporation, the cells were transferred to human AB serum supplemented IMDM with the previously indicated concentrations of M-CSF and TC or FBS supplemented DMEM, accordingly.

2.5. Immunoblotting

Mouse monoclonal antibody against MerTk was purchased from R&D systems (Minneapolis, USA) (MAB8911). Cells were collected and washed with PBS followed by lysing in 50 mM Tris–HCl; 0.1% Triton X-100; 1 mM EDTA; and 15 mM 2-MEA and proteinase inhibitors. Insoluble cellular material was removed by centrifugation and the lysates were mixed with 5× Laemmli loading buffer, boiled for 10 min and loaded onto a 8% SDS polyacrylamide gel. Proteins were transferred onto PVDF membranes followed by blocking with 5% skimmed milk. Membranes were probed by monoclonal anti-MerTk antibody (MAB8911, R&D systems) and β-actin (Sigma-Aldrich) overnight at 4 °C, followed by incubation with horseradish-peroxidase (HRP)-conjugated anti-mouse antibody (Sigma-Aldrich) for 1 h at room temperature. Immunoblots were developed with Immobilon Western chemiluminescent substrate (Millipore). Densitometry was carried out using ImageJ software.

2.6. Immunofluorescent staining and confocal microscopy

Macrophages were plated on 12 mm cover glass (1.5 × 106/well) and cultured as previously described. After co-culturing of the

Table 3
List of genes with significant expression changes in HMDMs during phagocytosis of ARPE-19 cells (Cont Assay vs Cont MΦ)(FC > 2; p < 0.05).

Downregulated genes	Gene description	FC	p-Value
BIRC1	NLR family, apoptosis inhibitory protein	0.11	0.0041
C1QA	Complement component 1, q subcomponent, A chain	0.12	0.0192
TNF	Tumor necrosis factor	0.12	0.0019
PTAFR	Platelet-activating factor receptor	0.14	0.0033
NALP12	NLR family, pyrin domain containing 12	0.16	0.0289
FCGR2B	Fc receptor, IgG, low affinity IIb	0.17	0.0339
C2	Complement component 2	0.18	0.0189
PECAM1	Platelet/endothelial cell adhesion molecule 1	0.19	0.0358
IRF4	Interferon regulatory factor 4	0.20	0.0232
ELMO1	Engulfment and cell motility 1	0.22	0.0466
IRF5	Interferon regulatory factor 5	0.24	0.0024
ITGAX	Integrin, alpha X (complement component 3 receptor 4 subunit)	0.24	0.0328
PTGER2	Prostaglandin E receptor 2 (subtype EP2), 53 kDa	0.24	0.0433
CASP1	Caspase 1	0.27	0.0288
ICAM3	Intercellular adhesion molecule 3	0.31	0.0350
PYCARD	PYD and CARD domain containing	0.40	0.0116
PPARG	Peroxisome proliferator-activated receptor gamma	0.41	0.0390
ELMO2	Engulfment and cell motility 2	0.46	0.0163
MERTK	c-Mer proto-oncogene tyrosine kinase	0.46	0.0371
ADORA3	Adenosine A3 receptor	0.48	0.0345
Highly upregulated genes			
ADORA1	Adenosine A1 receptor	109.70	0.0020
ANXA1	Annexin A1	84.64	0.0014
AXL	AXL receptor tyrosine kinase	80.02	0.0009
BCAR1	Breast cancer anti-estrogen resistance 1	58.34	0.0006
C4A	Complement component 4A (Rodgers blood group)	20.09	0.0071
Moderately upregulated genes			
CAPN1	Calpain 1, (mu/I) large subunit	16.86	0.0007
CAPN2	Calpain 2, (m/II) large subunit	12.72	0.0355
DNASE1	Deoxyribonuclease I	12.47	0.0028
DOCK1	Dedicator of cytokinesis 1	11.70	0.0014
GAS6	Growth arrest-specific 6	11.62	0.0040
GRLF1	Glucocorticoid receptor DNA binding factor 1	9.98	0.0041
GULP1	GULP, engulfment adaptor PTB domain containing 1	8.40	0.0077
IL18	Interleukin 18 (interferon-gamma-inducing factor)	6.40	0.0239
IRF1	Interferon regulatory factor 1	5.64	0.0238
IRF7	Interferon regulatory factor 7	5.11	0.0405
Slightly upregulated genes			
ITGAV	Integrin, alpha V	4.81	0.0022
MFGE8	Milk fat globule-EGF factor 8 protein	4.70	0.0010
PROS1	Protein S (alpha)	4.55	0.0084
PTK2	PTK2 protein tyrosine kinase 2	4.08	0.0290
PTX3	Pentraxin 3, long	3.78	0.0388
RAC1	Ras-related C3 botulinum toxin substrate 1 (rho family, Small GTP binding protein Rac1)	3.42	0.0022
THBS1	Thrombospondin 1	3.38	0.0064

macrophages with the dying cells for 4 h, the cells were washed and stained with anti-MerTk primary antibody (R&D systems) for 60 min on ice. NL-493 anti-mouse (R&D systems) was used as a secondary antibody before being washed and fixed in 4% paraformaldehyde for 10 min on ice. Images were taken with a Zeiss LSM 510 or Olympus FV1000 confocal laser scanning microscope. For visualizing the distribution of MerTk, overview images and three-dimensional stacks were acquired at 1-μm optical thickness. Three-dimensional reconstructions and x–y–z projections were created with the LSM 4.0 software. Images were processed and protein accumulation was determined by Fiji software as for positive events at least 20% of the total investigated protein exposed by a macrophage was clustered to the connecting points between phagocytes and dying ARPE-19 cells.

2.7. Statistical analysis

Statistical analysis of the phagocytosis data was performed by using the paired Student's *t*-test (two tailed). Statistical evaluation of the expression changes in comparison of two groups was performed in "R" using BioConductor implementing a moderate *t*-test based on Bayesian statistic which allows for a comparably reliable estimation of the SD even in the case of few biological replicates. For multiple comparisons of groups statistical significance was calculated and evaluated by one-way ANOVA.

3. Results

3.1. Induction of apopto-phagocytic genes in macrophages under triamcinolone treatment

Macrophages derived from human blood monocytes express all the necessary genes needed for carrying out efficient phagocytosis [17]. Using a self-designed apopto-phagocyte gene-array [17], gene expression changes were examined in control and TC-treated HMDMs during engulfment of anoikic ARPE-19 cells. Altogether significant changes in the expression of 56 out of the investigated 95 genes were found in multiple comparisons between the different groups and donors (Fig. 1, Table 1). The expression level of MFGE8, THSB1, ADORA3 and MERTK of the analyzed 95 genes increased significantly after TC treatment in HMDMs that are listed in Table 2. There was also a heterogenous group of genes with high level of expression in the macrophages that did not change during TC treatment (0.5 < FC < 2): ANXA5, CALR, CD68, and ITGB2.

3.2. Comparison of the gene expression patterns in macrophages from different donors with or without triamcinolone treatment: relative levels of gene expression in macrophages

The relative expressions of apopto-phagocytic genes in HMDMs of different donors were also compared. We observed that there were non-variable genes, whose relative expression level varied only 20% among donors (ADORA2B, ANXA1, ATG5, CD14, CIAS1, ELMO1, ICAM3, IL1B, IRF1, IRF5, ITGAM, ITGAV, ITGB3, PYCARD, TRIO), and there were highly variable ones, whose expression level varied in 2–3 orders of magnitude (ADORA1, ASGR1, CARD15, CD68, IL23A, IL6, MAP1LC3A, MFGE8, OLR1, TGM2, TYRO3) (data not shown). The expression level of the non-variable genes was typically higher and some of them were down-regulated upon TC treatment (ANXA1, ICAM3, IL1B, ITGAM, ITGB3). Based on these data, it can be assumed that these genes encode proteins that are essential to macrophage function and most of them are induced during TC treatment.

3.3. Effect of triamcinolone on the gene expression pattern of differentiated macrophages during engulfment of anoikic ARPE-19 cells

Engulfment of anoikic ARPE-19 cells resulted in significant expression changes in 43 out of the investigated 95 genes in the macrophages (Fig. 2), but in the case of ANXA5 the expression change did not reach the two-fold limit, therefore it does not appear in Table 3 (FC > 2, p < 0.05). CS treatment can highly increase the phagocytic capacity of macrophages toward anoikic RPE cells [26]. According to our data based on macrophages from a large number of donors in the presence of 1 μM TC, there is a 2-fold enhancement of the phagocytosis (n = 10, data not shown). As a result of TC treatment, ADORA3 and THBS1 were significantly upregulated as compared to macrophages grown in the absence of TC

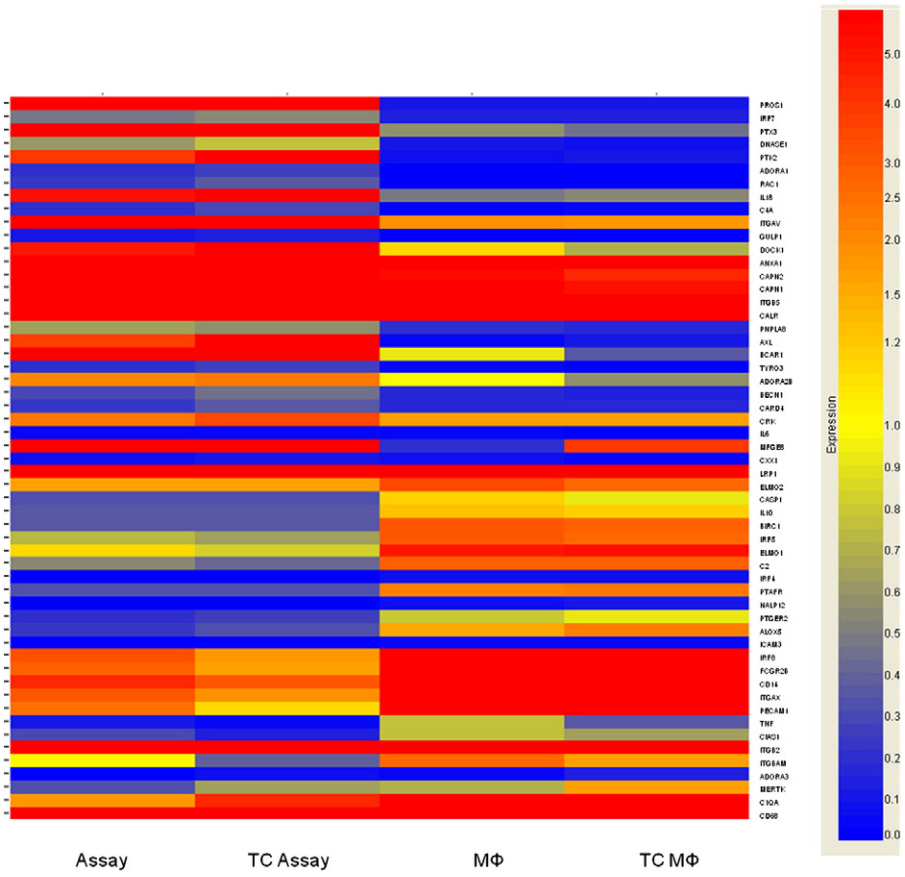

Fig. 3. Heatmap of the 55 out of the 95 genes investigated with significant changes upon assay conditions of TC-treated macrophages.

during engulfment of anoikic ARPE-19 cells (data not shown), while the expression of 55 genes altered significantly as compared to TC-treated macrophages (Fig. 3) out of which Table 4 shows the list of the genes with more than two times FC. The TC-induced genes encode either receptors (ADORA1, ADORA3, ALOX5, AXL, CALR, FCGR2B, ITGAM, ITGAV, ITGAX, ITGB2, ITGB5, LRP1, MERTK, PTGER2, PTK2, PTX3, TYRO3) or bridge-building proteins (ANXA1, C1QA, C2, C4A, ICAM3, MFGE8, PROS1) between phagocytes and apoptotic cells. It should be noted that 2 of them (ADORA1, MFGE8) were from the group of genes whose expression was quite variable among donors, and the other 17 of them (ADORA3, ALOX5, AXL, C1QA, C2, C4A, CALR, FCGR2B, ITGAX, ITGB2, ITGB5, LRP1, MERTK, PROS1, PTGER2, PTK2, PTX3) were in the intermediate group regarding their variance.

3.4. Functional effect of knocking-down of triamcinolone upregulated genes on phagocytosis

To investigate whether TC-induced upregulation had a direct effect on the enhanced phagocytic capacity of macrophages, a selection of the upregulated genes were silenced using siRNA. The transfection procedure did not cause significant loss of cells and did not have an adverse effect on the phagocytosis capacity (data not shown). The silencing efficiency of the target genes varied among different macrophage donors (Table 5) and replicates of living ARPE-19 cells (Table 6) as described previously [17]. Although the weakest silencing effect in macrophages was achieved for the members of TAM family (about 20–50%, Table 5) the phagocytosis of only the TC-treated MERTK and AXL knock-down macrophages decreased significantly (Fig. 4A). The combination of MERTK silencing with siRNAs for AXL (Fig. 4A) or any of the other TC upregulated genes as well as bridging molecules with each other (data not shown) did not show a significant synergistic effect. Furthermore, silencing of MERTK and AXL in living TC-treated ARPE-19 cells resulted in a significant decrease in non-professional clearance of anoikic ARPE-19 cells (Fig. 4B).

3.5. Pivotal role of the MerTk receptor in the TC-enhanced phagocytosis of dying ARPE-19 cells by macrophages

We also investigated whether blocking of MerTk with an antibody verifies its key role in TC-induced increase of phagocytosis. It was found that while the MerTk blocking antibody did not inhibit phagocytosis by macrophages differentiated in the absence of TC, the TC-induced increase of phagocytic capacity of macrophages could be prevented by treatment with this antibody (Fig. 5A). The distribution of the MerTk receptor on macrophages during engulfment of dying ARPE-19 cells in the presence or absence of TC is shown in Fig. 5B. MerTk was found in punctated structures at the cell borders of human macrophages and anoikic ARPE-19 cells, and it was accumulated at the connecting points between TC-treated macrophages and dying ARPE-19 cells in a larger extent that could be detected in 30–50% of the engulfment gates of three different macrophage donors (data not shown). Besides that, the expression of MerTk protein was confirmed by immunoblotting showing lower expression in both untreated cell types and much more elevated expression as a result of TC treatment in macrophages even during engulfment of anoikic ARPE-19 cells (Fig. 5C).

3.6. Impact of blocking MerTk on the TC-enhanced phagocytosis of dying ARPE-19 cells by living ARPE-19 cells

Furthermore, we wanted to learn whether blocking of MerTk with an antibody has an impact in the TC-induced increase of non-

Table 4
Phagocytosis effect on expression of apopto-phagocytic genes in TC-treated HMDMs (TC Assay vs TC MΦ)(FC > 2, p < 0.05).

Downregulated genes	Gene description	FC	p-Value
ADORA3	Adenosine A3 receptor	0.09	0.0175
ALOX5	Arachidonate 5-lipoxygenase	0.09	0.0082
BIRC1	NLR family, apoptosis inhibitory protein	0.11	0.0068
C1QA	Complement component 1, q subcomponent, A chain	0.12	0.0445
C2	Complement component 2	0.13	0.0002
CASP1	Caspase 1	0.13	0.0156
CD14	CD14 molecule	0.13	0.0229
CD68	CD68 molecule	0.14	0.0067
CIAS1	NLR family, pyrin domain containing 3	0.14	0.0051
ELMO1	Engulfment and cell motility 1	0.14	0.0026
FCGR2B	Fc receptor, IgG, low affinity IIb	0.14	0.0158
ICAM3	Intercellular adhesion molecule 3	0.15	0.0046
IL10	Interleukin 10	0.16	0.0016
IRF4	Interferon regulatory factor 4	0.19	0.0192
IRF5	Interferon regulatory factor 5	0.22	0.0312
IRF8	Interferon regulatory factor 8	0.23	0.0426
ITGAM	Integrin, alpha M (complement component 3 receptor 3 subunit)	0.24	0.0046
ITGAX	Integrin, alpha X (complement component 3 receptor 4 subunit)	0.25	0.0013
ITGB2	Integrin, beta 2 (complement component 3 receptor 3 and 4 subunit)	0.26	0.0040
MERTK	c-Mer proto-oncogene tyrosine kinase	0.28	0.0308
NALP12	NLR family, pyrin domain containing 12	0.29	0.0496
PECAM1	Platelet/endothelial cell adhesion molecule 1	0.31	0.0132
PTAFR	Platelet-activating factor receptor	0.35	0.0295
PTGER2	Prostaglandin E receptor 2 (subtype EP2), 53 kDa	0.37	0.0022
TNF	Tumor necrosis factor	0.50	0.0132
Highly upregulated genes			
PROS1	Protein S (alpha)	160.10	0.0028
PTK2	PTK2 protein tyrosine kinase 2	73.18	0.0001
AXL	AXL receptor tyrosine kinase	69.71	0.0002
BCAR1	Breast cancer anti-estrogen resistance 1	47.57	0.0022
RAC1	Ras-related C3 botulinum toxin substrate 1 (rho family, small GTP binding protein Rac1)	25.77	0.0002
TYRO3	TYRO3 protein tyrosine kinase 3	25.25	0.0059
ADORA1	Adenosine A1 receptor	24.80	0.0030
PTX3	Pentraxin 3, long	21.47	0.0110
Moderately upregulated genes			
C4A	Complement component 4A (Rodgers blood group)	18.13	0.0079
IL18	Interleukin 18 (interferon-gamma-inducing factor)	16.59	0.0002
ITGAV	Integrin, alpha V	16.48	0.0006
GULP1	GULP, engulfment adaptor PTB domain containing 1	12.72	0.0225
DOCK1	Dedicator of cytokinesis 1	10.98	0.0022
DNASE1	Deoxyribonuclease I	10.12	0.0090
ANXA1	Annexin A1	8.93	0.0011
CAPN2	Calpain 2, (m/II) large subunit	8.49	0.0032
CAPN1	Calpain 1, (mu/I) large subunit	5.35	0.0041
MFGE8	Milk fat globule-EGF factor 8 protein	5.34	0.0168
Slightly upregulated genes			
IRF7	Interferon regulatory factor 7	4.64	0.0069
ADORA2B	Adenosine A2b receptor	4.34	0.0095
IL6	Interleukin 6 (interferon, beta 2)	4.13	0.0078
ITGB5	Integrin, beta 5	3.38	0.0163
PNPLA8	Patatin-like phospholipase domain containing 8	3.34	0.0029
BECN1	Beclin 1, autophagy related	3.10	0.0313
CALR	Calreticulin	3.01	0.0198
CXXC1	CXXC finger protein 1	2.61	0.0179
CARD4	Nucleotide-binding oligomerization domain containing 1	2.35	0.0102
CRK	v-Crk sarcoma virus CT10 oncogene homolog (avian)	2.11	0.0456

professional phagocytosis performed by living ARPE-19 cells. We observed that while the MerTk blocking antibody did not inhibit phagocytosis by non-professional phagocytes in the absence of TC (data not shown), their TC-enhanced phagocytic capacity could be significantly decreased by treatment with this antibody administered either on the side of the phagocytes or to the anoikic ARPE-19 cells (Fig. 6A). MerTk was also found in punctated structures at the cell borders of phagocytosing ARPE-19 cells, and it was accumulated at the engulfment portals between TC-treated phagocytes and dying ARPE-19 cells in a larger extent (Fig. 6B) that could be detected in 20–40% of the engulfment gates of three different replicates (data not shown). The expression of MerTk protein was visualized by immunoblotting showing lower expression in TC untreated cells and much more elevated expression as a result of the

Table 5
Numerical data of the silencing effect on apopto-phagocytic genes in macrophages showing the biological variance of different donors. Gene expression level of TC upregulated apopto-phagocytic genes after silencing in 5 different macrophage donors (in percent as compared to TC-treated Mock).

Silenced gene expression%					
Gene name	Donor no. 1	Donor no. 2	Donor no. 3	Donor no. 4	Donor no. 5
ADORA 3	19.56	15.07	–	–	–
AXL	58.91	26.86	1.89	0.67	27.47
MERTK	27.64	56.80	4.41	28.15	60.54
THBS1	8.51	28.58	–	–	–

Table 6
Numerical data of the silencing effect on apopto-phagocytic genes in living ARPE-19 cells. Gene expression level of AXL and MERTK genes after silencing in 5 different biological replicates (in percent as compared to TC-treated Mock).

Silenced gene expression%					
Gene name	Donor no. 1	Donor no. 2	Donor no. 3	Donor no. 4	Donor no. 5
AXL	20.96	16.84	1.89	–	–
MERTK	1.11	14.87	11.43	55.11	44.91

engulfment process even during TC treatment of the phagocytosing ARPE-19 cells (Fig. 6C). In parallel, the expression of MERTK and AXL genes in living ARPE-19 cells slightly increased upon TC treatment while they show a significantly elevated expression during the engulfment of anoikic ARPE-19 cells in TC-treated non-professional phagocytes (data not shown).

3.7. Functional effect of blocking and augmentation of MerTk in the clearance of primary human RPE cells by macrophages

In addition, we intended to establish an ex vivo model studying the effect of TC treatment on the clearance of human primary RPE cells by professional phagocytes. In our study, TC treatment of macrophages 48 h prior the phagocytic assay enhanced the macrophage-mediated clearance of dying retinal cells: an augmentation of about 1.5–2 times in the engulfing capacity of anoikic hRPE cells occurred at 4 h of co-incubation (Fig. 7A). The administration of blocking antibody acting on MerTk significantly reduced the engulfment of dying hRPE cells by TC-treated macrophages (Fig. 7B) similarly to the in vitro clearance model of anoikic dying ARPE-19 cells described previously. Finally, we wanted to learn whether the augmentation of MerTk by its ligand, the bridging molecule Gas6 can affect the clearance of anoikic ARPE-19 and hRPE cells. Untreated macrophages moderately increased their phagocytosis capacity upon Gas6 treatment, while a remarkable phagocytosis enhancing effect was found in a concentration dependent manner in the case of TC-treated macrophages (Fig. 7C, D) in which MerTk was significantly overexpressed both at mRNA (Table 2) and protein level (Fig. 5C).

4. Discussion

In this study gene expression pattern changes are defined by TLDA in control and TC-treated HMDMs before and during engulfment of anoikic ARPE-19 cells. Our data show that the phagocytes in their pre-phagocytic state are equipped with a full array of apopto-phagocytic genes which can be highly upregulated. TC treatment itself leads to a significant upregulation of 4 genes: MFGE8, THBS1, ADORA3 and MERTK, while the engulfment of anoikic ARPE-19 cells results in upregulation (FC > 2) of 22 genes among which are AXL, MFGE8, ITGAV, GAS6 and THBS1. Interestingly, engulfment of anoikic ARPE-19 cells by TC pre-treated HMDMs leads to a significant upregulation of 27 genes, also including AXL, MFGE8, ITGAV, GAS6, THBS1 as well as ADORA3 (although, the FC did not reach the 2-fold limit in case of ADORA3). MERTK was upregulated by the TC treatment, but it was downregulated during the engulfment of anoikic ARPE-19 cells by nontreated macrophages and also during phagocytosis in TC-treated macrophages; the difference overall was slightly higher expression of the MERTK in the TC treated compared to the nontreated phagocytosing macrophages. The expression pattern of ADORA3 was similar to the one of MERTK. MFGE8, THBS1 and GAS6 also had some similarities, but the main difference was that they were always upregulated compared to the nontreated, nonphagocytosing macrophages. AXL and ITGAV expressions were increased with TC treatment, and it further increased during phagocytosis reaching the highest expression during engulfment by TC pre-treated macrophages.

Based upon our TLDA results, it can be argued that out of the 43 genes that significantly changed during the engulfment of anoikic ARPE-19 cells by non-treated macrophages, there are 36 common or overlapping genes with the 55 genes which significantly changed during phagocytosis in TC pre-treated macrophages. Out of these 36 genes, only the expression of 3 genes (ADORA3, MERTK, MFGE8) had changed significantly by the TC treatment in non-phagocytosing macrophages. Furthermore, only silencing of MERTK and AXL could prevent TC-mediated increase in phagocytosis of anoikic ARPE-19 cells, which has been further confirmed by applying blocking antibodies against MerTk.

It is widely accepted that immunologic processes are involved in the pathogenesis of AMD, including the generation of inflammatory related molecules in Bruch's membrane, recruitment of macrophages, dendritic cells (DCs), complement activation and microglial activation in the macular area [28–31]. Disturbance of the immunological processes may lead to detrimental protein aggregation and RPE cell death. Non-professional (living RPE cells) and professional phagocytes (macrophages and DCs), thus have a central role in the development of AMD.

Non-professional phagocytosis by RPE cells is usually linked to the regulation of a normal visual cycle. RPE cells are responsible for the diurnal photoreceptor outer segment (POS) clearance as first documented in the 1960's [32]. The renewal or recycling of the POSs with the help of RPE is essential for the survival of rods and cones, and diminished phagocytic capacity of RPE cells has been associated with degenerative diseases of the retina including AMD [29,33]. Phagocytosis of the POS

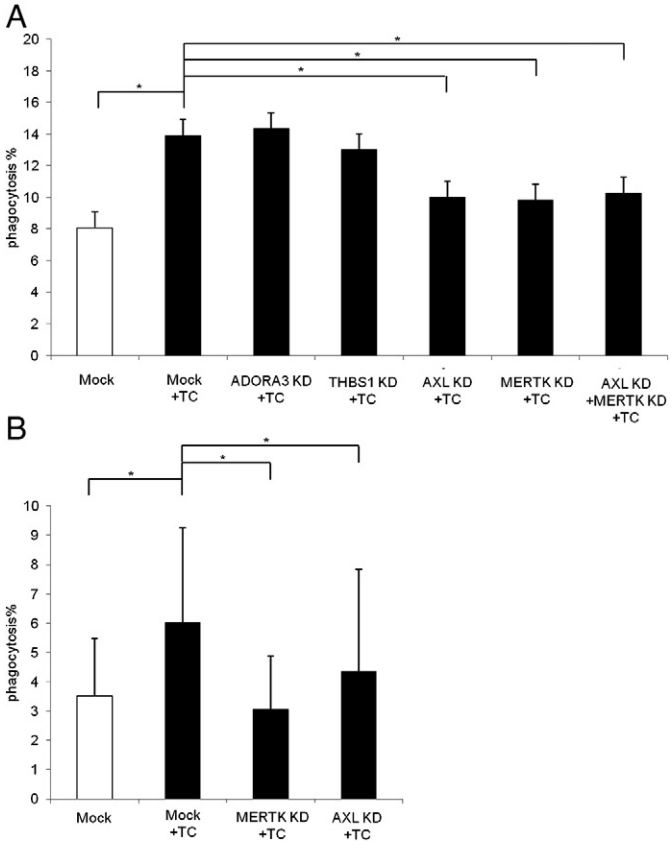

Fig. 4. *Functional effect of knocking-down of triamcinolone upregulated genes on professional and non-professional phagocytosis.* (A) Phagocytosis of anoikic ARPE-19 cells by macrophages after knocking down TC upregulated apopto-phagocytic genes. Genes silenced by specific siRNA: ADORA3, THBS1, AXL, MERTK (n = 5) or AXL and MERTK simultaneously (n = 3). Black bars represent TC-treated macrophages; *p < 0.05. (B) Phagocytosis of anoikic ARPE-19 cells by living ARPE-19 cells after knocking down AXL and MERTK genes. Black bars represent TC-treated phagocytes; *p < 0.05, n = 5.

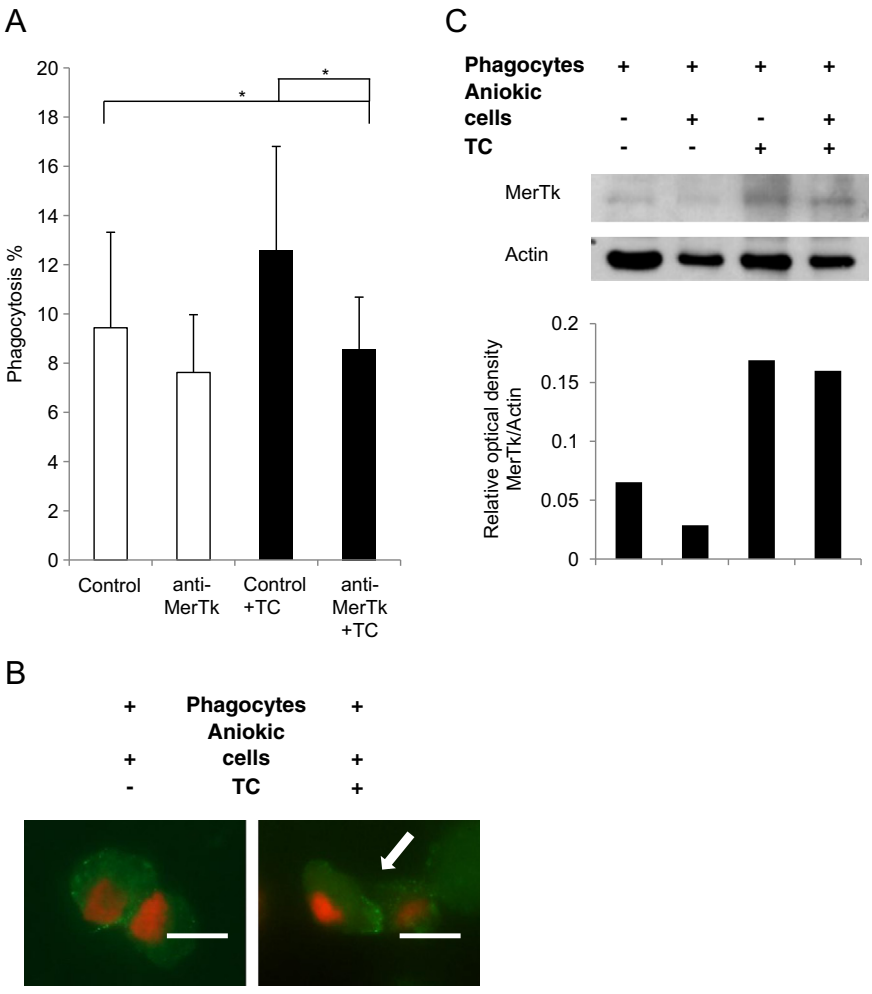

Fig. 5. *Impact of blocking of Mertk receptor on the phagocytosis of dying ARPE-19 cells by macrophages* (A) Phagocytosis of anoikic ARPE-19 cells by macrophages after blocking of Mertk on the surface of macrophages by specific antibody. Black bars represent TC-treated macrophages; $^{*}p < 0.05$, n = 4. (B) Localization of Mertk during recognition of dying ARPE-19 cells by macrophages with or without TC treatment. Images were taken with a Zeiss LSM 510 fluorescent microscope. Bars represent 5 μm. Arrow indicates clustering of Mertk at the engulfment portals of macrophages. (C) Western blot analysis of Mertk expression in one representative macrophage donor that engulf anoikic ARPE-19 cells with or without TC treatment. Relative optical density was determined by densitometry using ImageJ software.

occurs at the apical side of the RPE cells, which is intimately associated with the photoreceptor layer. Once the disks have been internalized, the phagosome moves from the apical to the basal surface where the contents of the phagosome become degraded. A failure in phagocytosis during aging leads to accumulation of protein aggregates, retinal degeneration and finally photoreceptor cell death [34]. The MerTk expressed by RPE cells has been observed to be a key protein in the regulation of POS phagocytosis [35,36]. Regulation of phagocytosis is a complex process involving recognition and attachment of the POS disks, their ingestion, formation of the phagosome and its fusion with the lysosomes, and degradation [37]. The expression of ITGAV ($\alpha v\beta 5$ integrin) on the apical side of the RPEs is required for binding of POS [38,39]. A milk fat globule-EGF8 (MFG-E8), a ligand of the ITGAV regulates the circadian rhythm of phagocytosis [39,40]. MerTk is activated by ITGAV receptors and these are required for POS clearance [41]. During the aging process, the reduction in ITGAV levels leads to an accumulation of the harmful lysosomal lipofuscin in the RPE that secondarily evokes vision loss [42,43].

Our recent findings reveal that the non-professional RPE cells are able to clean larger apoptotic or anoikic cells in addition to POS material [26]. However, it is poorly known how POS or dying cells' phagocytosis differs in their signaling cascades between non-professional and professional phagocytes in the retina. For example, it has been documented that macrophages and DCs use different receptors for phagocytosis [44]. As far as we are aware, this is the first study showing the role of MerTk in the regulation of TC-enhanced phagocytosis not only in non-professional RPE cells but also in professional phagocytes. To strengthen the role of TC in the different stages of phagocytosis, increased expression of MFG-E8, ITGAV, TYRO3, AXL and THSB-1 genes was observed in the macrophages treated by TC.

A total of 80% of all patients suffering from AMD have the dry form of the disease for which no efficient treatment exists today. In dry AMD, the clearance process is mainly based upon non-professional phagocytosis [29]. In the neovascular (NV) or wet type of AMD, new vessels sprout from the choroidal capillaries through the Bruch's membrane into the sub-RPE space or into the retinal layers. A thickening, calcification, and fragmentation of Bruch's membrane may predispose to the development of choroidal neovascular membranes (CNVs) from the choriocapillaris to the retina. These detrimental new blood vessels are diagnostic hallmark for wet AMD and they usually get disrupted and leak blood or fluid into the subretinal pigment epithelial space, eventually evoking fibrogliosis which results in a disciform scar formation and severe visual loss if not treated properly. Wet AMD development is strongly associated with the recruitment and activation of professional phagocytes and upregulation of vascular endothelial growth factor (VEGF) [2,26,45]. To date, VEGF is the principal therapy target for

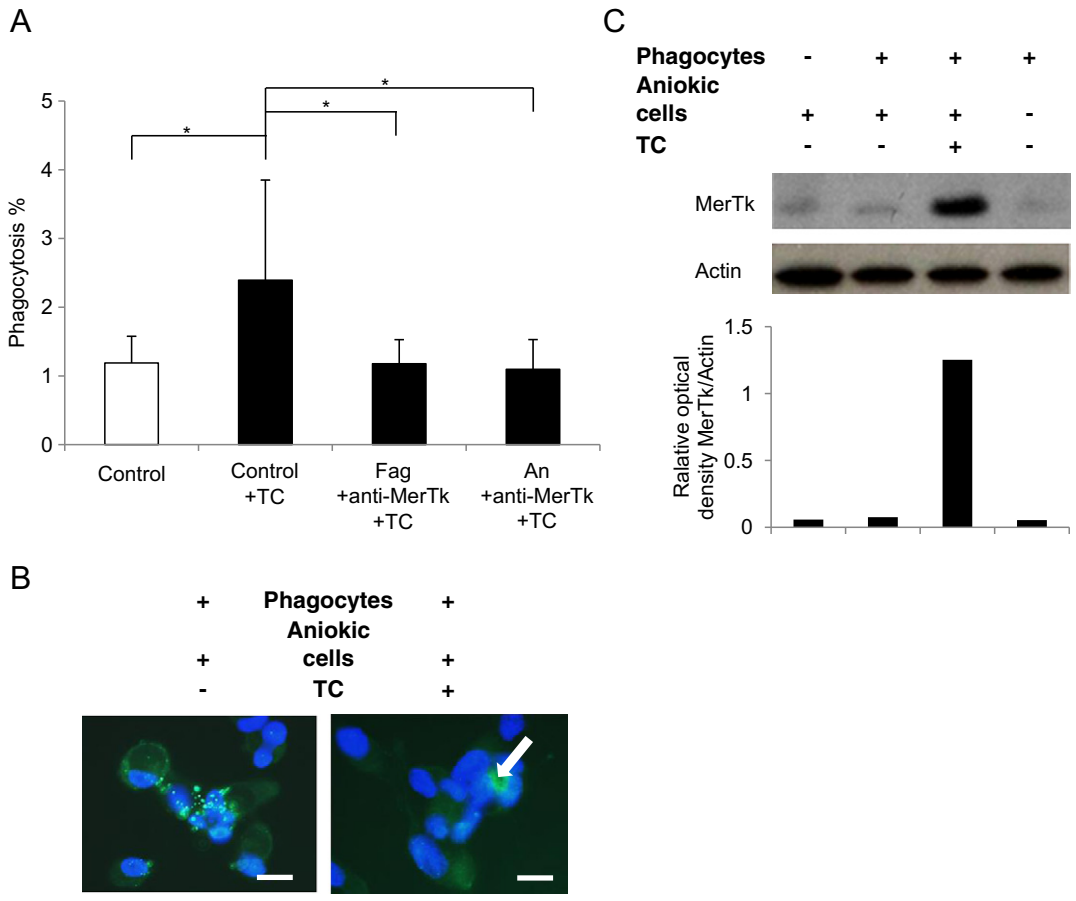

Fig. 6. *Impact of blocking Mertk receptor on the phagocytosis of dying ARPE-19 cells by non-professional phagocytes* (A) Phagocytosis of anoikic ARPE-19 cells by living ARPE-19 cells after blocking of Mertk on the surface of living and dying ARPE-19 cells by specific antibody. Black bars represent TC-treated phagocytes; *$p < 0.05$, $n = 4$. (B) Localization of Mertk during recognition of dying ARPE-19 cells by living ARPE-19 cells with or without TC treatment. Images were taken with a Zeiss LSM 510 fluorescent microscope. Bars represent 5 μm. Arrow indicates clustering of Mertk at the engulfment portals of non-professional phagocytes. (C) Western blot analysis of Mertk expression in living and dying ARPE-19 cells and even during engulfment of anoikic ARPE-19 cells with or without TC treatment. Relative optical density was determined by densitometry using ImageJ software.

inhibiting the detrimental neovascularization process by intravitreal administration of ranibizumab, bevacizumab or VEGF Trap [46–48]. Patients with wet AMD, in whom monotherapy with anti-VEGF was unsuccessful, may experience a temporary improvement in vision and reduction in macular thickness after a combined intravitreal injection of bevacizumab and TC [49].

In this study, we clearly show that TC treatment enhances phagocytosis via the MerTk signaling pathway in both non-professional and professional phagocytes. Regulation of retinal phagocytosis by TC, which has anti-inflammatory and anti-fibrotic capacity, may open new possibilites to treat different AMD phenotypes. In addition, experiments with primary RPE give an opportunity to investigate AMD ex vivo under in vivo-like conditions. In particular, the use of Gas6 as enhancer of retinal phagocytosis via the MerTK receptor, alone or in combination with other specific ligands of the tyrosine kinase receptors' family may serve as future targets for AMD therapy.

Acknowledgement

Funding: The study has been funded by a grant from the Hungarian Scientific Research Fund (OTKA PD 101316) and TÁMOP-4.2.4.A/2-11-1-2012-0001 'National Excellence Program' provided personal support to E.K. The funders had no role in the study design, data collection and analysis, decision to publish, or preparation of the manuscript.

Appendix A. Supplementary data

Supplementary data to this article can be found online at http://dx.doi.org/10.1016/j.bbagen.2014.10.026.

References

[1] W.R. Green, C. Enger, Age-related macular degeneration histopathologic studies. The 1992 Lorenz E. Zimmerman Lecture, Ophthalmology 100 (1993) 1519–1535.
[2] J.V. Forrester, Macrophages eyed in macular degeneration, Nat. Med. 9 (2003) 1350–1351.
[3] E.U. Irschick, R. Sgonc, G. Bock, H. Wolf, D. Fuchs, W. Nussbaumer, W. Gottinger, H.P. Huemer, Retinal pigment epithelial phagocytosis and metabolism differ from those of macrophages, Ophthalmic Res. 36 (2004) 200–210.
[4] J. Savill, I. Dransfield, C. Gregory, C. Haslett, A blast from the past: clearance of apoptotic cells regulates immune responses, Nat. Rev. Immunol. 2 (2002) 965–975.
[5] L.M. Stuart, R.A. Ezekowitz, Phagocytosis: elegant complexity, Immunity 22 (2005) 539–550.
[6] K. Lauber, S.G. Blumenthal, M. Waibel, S. Wesselborg, Clearance of apoptotic cells: getting rid of the corpses, Mol. Cell 14 (2004) 277–287.
[7] S.J. Gardai, D.L. Bratton, C.A. Ogden, P.M. Henson, Recognition ligands on apoptotic cells: a perspective, J. Leukoc. Biol. 79 (2006) 896–903.
[8] G. Májai, G. Petrovski, L. Fésüs, Inflammation and the apopto-phagocytic system, Immunol. Lett. 104 (2006) 94–101.
[9] L.P. Erwig, P.M. Henson, Clearance of apoptotic cells by phagocytes, Cell Death Differ. 15 (2007) 243–250.
[10] R.P. Danis, T.A. Ciulla, L.M. Pratt, W. Anliker, Intravitreal triamcinolone acetonide in exudative age-related macular degeneration, Retina 20 (2000) 244–250.
[11] N. Floman, U. Zor, Mechanism of steroid action in ocular inflammation: inhibition of prostaglandin production, Invest. Ophthalmol. Vis. Sci. 16 (1977) 69–73.

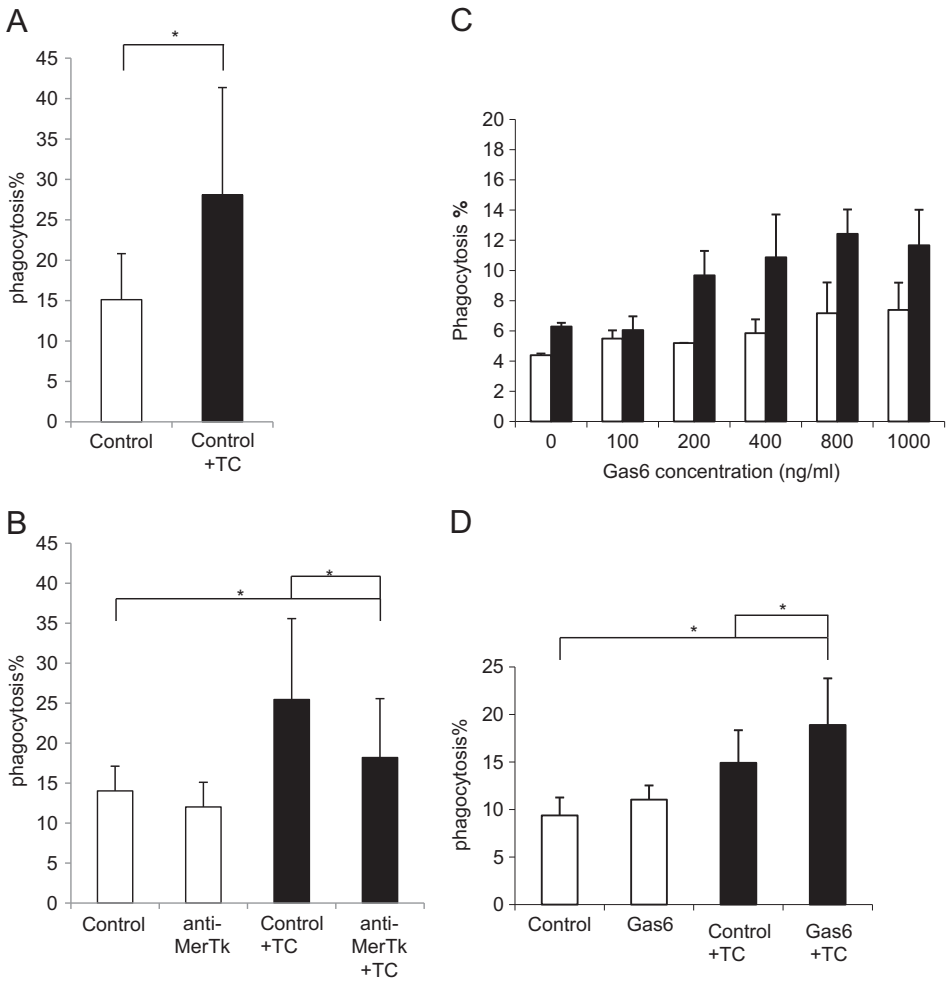

Fig. 7. *Impact of blocking and augmentation of Mertk receptor on the phagocytosis of dying human primary RPE cells by macrophages.* (A) Phagocytosis of anoikic hRPE cells by macrophages with or without TC treatment. Black bar represents TC-treated macrophages; *$p < 0.05$, $n = 7$. (B) Phagocytosis of dying hRPE cells by macrophages after blocking of Mertk on the surface of macrophages by specific antibody. Black bars represent TC-treated macrophages; *$p < 0.05$, $n = 4$. (C) Engulfment of dying ARPE-19 cells by macrophages after augmentation of Mertk on the surface of macrophages by the bridging molecule Gas6. Black bars represent TC-treated macrophages. Results showing phagocytosis capacity of one representative macrophage donor. SD means the experimental error of the technical replicates. (D) Phagocytosis of anoikic hRPE cells by macrophages after augmentation of Mertk on the surface of macrophages by Gas6. Black bars represent TC-treated macrophages; *$p < 0.05$, $n = 4$.

[12] G.D. Lewis, W.B. Campbell, A.R. Johnson, Inhibition of prostaglandin synthesis by glucocorticoids in human endothelial cells, Endocrinology 119 (1986) 62–69.
[13] J.A. Ford, N. Lois, P. Royle, C. Clar, D. Shyangdan, N. Waugh, Current treatments in diabetic macular oedema: systematic review and meta-analysis, BMJ Open 3 (2013).
[14] J.B. Jonas, I. Akkoyun, I. Kreissig, R.F. Degenring, Diffuse diabetic macular oedema treated by intravitreal triamcinolone acetonide: a comparative, non-randomised study, Br. J. Ophthalmol. 89 (2005) 321–326.
[15] C. Stahn, M. Löwenberg, D.W. Hommes, F. Buttgereit, Molecular mechanisms of glucocorticoid action and selective glucocorticoid receptor agonists, Mol. Cell. Endocrinol. 275 (2007) 71–78.
[16] J.G. Tasker, S. Di, R. Malcher-Lopes, Minireview: rapid glucocorticoid signaling via membrane-associated receptors, Endocrinology 147 (2006) 5549–5556.
[17] G. Zahuczky, E. Kristóf, G. Majai, L. Fésüs, Differentiation and glucocorticoid regulated apopto-phagocytic gene expression patterns in human macrophages. Role of Mertk in enhanced phagocytosis, PLoS One 6 (2011) e21349.
[18] G. Zizzo, P.L. Cohen, IL-17 stimulates differentiation of human anti-inflammatory macrophages and phagocytosis of apoptotic neutrophils in response to IL-10 and glucocorticoids, J. Immunol. 190 (2013) 5237–5246.
[19] G. Zizzo, B.A. Hilliard, M. Monestier, P.L. Cohen, Efficient clearance of early apoptotic cells by human macrophages requires M2c polarization and MerTK induction, J. Immunol. 189 (2012) 3508–3520.
[20] K.M. Giles, K. Ross, A.G. Rossi, N.A. Hotchin, C. Haslett, I. Dransfield, Glucocorticoid augmentation of macrophage capacity for phagocytosis of apoptotic cells is associated with reduced p130Cas expression, loss of paxillin/pyk2 phosphorylation, and high levels of active Rac, J. Immunol. 167 (2001) 976–986.
[21] D.M. Mosser, The many faces of macrophage activation, J. Leukoc. Biol. 73 (2003) 209–212.
[22] J. Ehrchen, L. Steinmüller, K. Barczyk, K. Tenbrock, W. Nacken, M. Eisenacher, U. Nordhues, C. Sorg, C. Sunderkötter, J. Roth, Glucocorticoids induce differentiation of a specifically activated, anti-inflammatory subtype of human monocytes, Blood 109 (2007) 1265–1274.
[23] A. McColl, S. Bournazos, S. Franz, M. Perretti, B.P. Morgan, C. Haslett, I. Dransfield, Glucocorticoids induce protein S-dependent phagocytosis of apoptotic neutrophils by human macrophages, J. Immunol. 183 (2009) 2167–2175.
[24] R.S. Scott, E.J. McMahon, S.M. Pop, E.A. Reap, R. Caricchio, P.L. Cohen, H.S. Earp, G.K. Matsushima, Phagocytosis and clearance of apoptotic cells is mediated by MER, Nature 411 (2001) 207–211.
[25] S. Johnen, Z. Izsvák, M. Stöcker, N. Harmening, A.K. Salz, P. Walter, G. Thumann, Sleeping Beauty transposon-mediated transfection of retinal and iris pigment epithelial cells, Invest. Ophthalmol. Vis. Sci. 53 (2012) 4787–4796.
[26] G. Petrovski, E. Berenyi, M. Moe, A. Vajas, L. Fésüs, A. Berta, A. Facskó, Clearance of dying ARPE-19 cells by professional and nonprofessional phagocytes in vitro — implications for age-related macular degeneration (AMD), Acta Ophthalmol. 89 (2011) e30–e34.
[27] H. Fujimoto, K. Kato, H. Iwata, Layer-by-layer assembly of small interfering RNA and poly(ethyleneimine) for substrate-mediated electroporation with high efficiency, Anal. Bioanal. Chem. 397 (2010) 571–578.
[28] G.S. Hageman, P.J. Luthert, N.H. Victor Chong, L.V. Johnson, D.H. Anderson, R.F. Mullins, An integrated hypothesis that considers drusen as biomarkers of immune-mediated processes at the RPE-Bruch's membrane interface in aging and age-related macular degeneration, Prog. Retin. Eye Res. 20 (2001) 705–732.
[29] K. Kinnunen, G. Petrovski, M.C. Moe, A. Berta, K. Kaarniranta, Molecular mechanisms of retinal pigment epithelium damage and development of age-related macular degeneration, Acta Ophthalmol. 90 (2012) 299–309.
[30] P.L. Penfold, J.M. Provis, J.H. Furby, P.A. Gatenby, F.A. Billson, Autoantibodies to retinal astrocytes associated with age-related macular degeneration, Graefes Arch. Clin. Exp. Ophthalmol. 228 (1990) 270–274.
[31] J. Tuo, S. Grob, K. Zhang, C.-C. Chan, Genetics of immunological and inflammatory components in age-related macular degeneration, Ocul. Immunol. Inflamm. 20 (2012) 27–36.
[32] R.W. Young, D. Bok, Participation of the retinal pigment epithelium in the rod outer segment renewal process, J. Cell Biol. 42 (1969) 392–403.

[33] G.H. Travis, M. Golczak, A.R. Moise, K. Palczewski, Diseases caused by defects in the visual cycle: retinoids as potential therapeutic agents, Annu. Rev. Pharmacol. Toxicol. 47 (2007) 469–512.
[34] N. Rodríguez-Muela, H. Koga, L. García-Ledo, P. de la Villa, E.J. de la Rosa, A.M. Cuervo, P. Boya, Balance between autophagic pathways preserves retinal homeostasis, Aging Cell 12 (3) (2013) 478–488.
[35] M.H. Chaitin, M.O. Hall, Defective ingestion of rod outer segments by cultured dystrophic rat pigment epithelial cells, Invest. Ophthalmol. Vis. Sci. 24 (1983) 812–820.
[36] P.M. D'Cruz, D. Yasumura, J. Weir, M.T. Matthes, H. Abderrahim, M.M. LaVail, D. Vollrath, Mutation of the receptor tyrosine kinase gene Mertk in the retinal dystrophic RCS rat, Hum. Mol. Genet. 9 (2000) 645–651.
[37] E. Bosch, J. Horwitz, D. Bok, Phagocytosis of outer segments by retinal pigment epithelium: phagosome–lysosome interaction, J. Histochem. Cytochem. 41 (1993) 253–263.
[38] E.F. Nandrot, Y. Kim, S.E. Brodie, X. Huang, D. Sheppard, S.C. Finnemann, Loss of synchronized retinal phagocytosis and age-related blindness in mice lacking αvβ5 integrin, J. Exp. Med. 200 (2004) 1539–1545.
[39] E.F. Nandrot, M. Anand, D. Almeida, K. Atabai, D. Sheppard, S.C. Finnemann, Essential role for MFG-E8 as ligand for αvβ5 integrin in diurnal retinal phagocytosis, Proc. Natl. Acad. Sci. U. S. A. 104 (2007) 12005–12010.
[40] S. Finnemann, E. Nandrot, Mertk Activation During RPE Phagocytosis in Vivo Requires αVβ5 Integrin, in: J. Hollyfield, R. Anderson, M. LaVail (Eds.), Retinal Degenerative Diseases, vol. 572, Springer, New York, 2006, pp. 499–503.
[41] W. Feng, D. Yasumura, M.T. Matthes, M.M. LaVail, D. Vollrath, Mertk triggers uptake of photoreceptor outer segments during phagocytosis by cultured retinal pigment epithelial cells, J. Biol. Chem. 277 (2002) 17016–17022.
[42] M. Mallavarapu, S.C. Finnemann, Neural retina and MerTK-independent apical polarity of αvβ5 integrin receptors in the retinal pigment epithelium, Adv. Exp. Med. Biol. 664 (2010) 123–131.
[43] M. Mallavarapu, S. Finnemann, Neural Retina and MerTK-independent Apical Polarity of αvβ5 Integrin Receptors in the Retinal Pigment Epithelium, in: R.E. Anderson, J.G. Hollyfield, M.M. LaVail (Eds.), Retinal Degenerative Diseases, vol. 664, Springer, New York, 2010, pp. 123–131.
[44] H.M. Seitz, T.D. Camenisch, G. Lemke, H.S. Earp, G.K. Matsushima, Macrophages and dendritic cells use different Axl/Mertk/Tyro3 receptors in clearance of apoptotic cells, J. Immunol. 178 (2007) 5635–5642.
[45] A. Klettner, J. Roider, Mechanisms of Pathological VEGF Production in the Retina and Modification with VEGF-antagonists, in: R.D. Stratton, W.W. Hauswirth, T.W. Gardner (Eds.), Studies on Retinal and Choroidal Disorders, Humana Press, New York, 2012, pp. 277–305.
[46] U. Chakravarthy, S.P. Harding, C.A. Rogers, S.M. Downes, A.J. Lotery, S. Wordsworth, B.C. Reeves, Ranibizumab versus bevacizumab to treat neovascular age-related macular degeneration: one-year findings from the IVAN randomized trial, Ophthalmology 119 (2012) 1399–1411.
[47] J.S. Heier, D. Boyer, Q.D. Nguyen, D. Marcus, D.B. Roth, G. Yancopoulos, N. Stahl, A. Ingerman, R. Vitti, A.J. Berliner, K. Yang, D.M. Brown, The 1-year results of CLEAR-IT 2, a phase 2 study of vascular endothelial growth factor trap-eye dosed as-needed after 12-week fixed dosing, Ophthalmology 118 (2011) 1098–1106.
[48] D. Martin, M. Maguire, G.-S. Ying, J.E. Grunwald, S.L. Fine, G.J. Jaffe, Ranibizumab and bevacizumab for neovascular age-related macular degeneration, N. Engl. J. Med. 364 (2011) 1897–1908.
[49] Y. Tao, J.B. Jonas, Intravitreal bevacizumab combined with intravitreal triamcinolone for therapy-resistant exudative age-related macular degeneration, J. Ocul. Pharmacol. Ther. 26 (2010) 207–212.